Biosystems Engineering (2005) **90** (3), 319–330
doi:10.1016/j.biosystemseng.2004.12.001
SE—Structures and Environment

Effects of a Solar Desalination Module integrated in a Greenhouse Roof on Light Transmission and Crop Growth

M.T. Chaibi[1]; T. Jilar[2]

[1]Institut National de Recherche en Génie Rural, Eaux et Forets, B P 10, 2080 Ariana, Tunisia; e-mail of corresponding author: chaibi.medthameur@iresa.agrinet.tn
[2]Swedish University of Agricultural Sciences, P O Box 86, 230 53 Alnarp, Sweden; e-mail: torbjorn.jilar@jbt.slu.se

(Received 27 December 2002; accepted in revised form 1 December 2004; published online 5 February 2005)

In greenhouses with roof-integrated water desalination, solar transmission is reduced by an absorbing glass sheet covered by a layer of flowing water and a top glass sheet. In this study, the main objective was to analyse differences in seasonal crop yields between greenhouses with desalination and conventional roofs in arid climates. A simulation model of the thermal and optical performance of this system is detailed as well as laboratory experiments. This model was combined with a lettuce growth model.

Simulation of the spectral transmission of photosynthetically active radiation (PAR), with and without water flow, was validated through laboratory experiments. A sensitivity analysis of the influence of the optical parameters on the transmission of the accumulated PAR and on crop yield for the complete solar desalination roof greenhouse are shown to give adequate representation of the relationships between light transmission and seasonal crop yield production sufficient to produce design guidelines for the desalination concept manufacturers or growers.

1. Introduction

There are conditions, especially during hot periods, when it is necessary to reduce the light transmission into the greenhouse. For these conditions, growers normally use thermal screens to limit plant temperature and avoid water stress resulting from high irradiation (Nijskens *et al.*, 1985).

The integrated greenhouse roof desalination system, previously analysed through simulation and experiments by Chaibi (2000, 2002), could be used as a thermal screen as well as a means for supplying irrigation water to greenhouse crops in arid areas (*Fig. 1*).

The limitation of solar radiation transmission into a greenhouse equipped with an integrated solar desalination system in the roof is of high importance for the transpiration and growth of the crop (Baille *et al.*, 1990). The quality of the transmitted light also could be significantly modified by the optical properties of the roof system resulting in photo-morphological effects on the plants. Consequently, the light quantity and quality could be limiting factors for crop growth, implying that designers of that such greenhouses must pay careful attention to the optical characteristics of the roof.

The installation of this type of system also means that higher investment costs should be balanced against lower water costs when compared to a more simple and conventional greenhouse solution. For such a system applied to commercial production, light and yield losses should be considered in a complete economical assessment (Holder & Cockshull, 1990; Cockshull *et al.*, 1992). A key factor of the economic evaluation is the use of more advanced, light selective and probably also more expensive materials in the future. Hence, the economical feasibility of the system will probably require simple and quite cheap structural solutions for the roof desalination system.

1.1. *Literature review*

Plants in protected cultivation respond in various ways to the reduction of the natural light level and

Notation

l	thickness, m	*Subscripts*	
n	index of refraction, dimensionless	a	air
r	reflection coefficient, dimensionless	ab	absorption
α	absorption coefficient, dimensionless	g	glass
β	extinction coefficient, m^{-1}	i	single layer
λ	wavelength, m	NIR	near infrared radiation
θ	angle between surface normal and incident beam radiation, deg	pa	parallel component of polarised radiation
τ	transmission coefficient for specific wavelength interval, dimensionless	pe	perpendicular component of polarised radiation
τ_{al}	transmission coefficient—absorption losses only, dimensionless	PAR	photosynthetically active radiation
τ_{rl}	transmission coefficient—reflection losses only, dimensionless	t	total
		UV	ultra violet radiation
		w	water

changes of its spectral composition (Raviv, 1989; McMahon *et al.*, 1990; Mortensen & Stromme, 1987). Understanding these responses is essential in order to design and control the operation of the roof desalination system, and to achieve optimal conditions in terms of plant growth, yield and disease control.

Measurements and models of the solar radiation transmission and spectral composition for greenhouse covering materials have been frequently reported subjects for many years (Baille *et al.*, 1987, 1990; Kozai, 1977; Critten, 1983; Pieters, 1996). However, very few results are reported concerning materials specifically used in desalination applications. Tinault *et al.* (1978) presented a compilation of the spectral solar transmission characteristics for sheets of coloured plastic materials, considered for roof-integrated desalination. He found that a maximal photosynthetic activity is obtained for red methacrylate sheets. Selcuk (1970) performed a theoretical analysis of the thermal balance for a still installed on a greenhouse roof and characterised the shading effect on the greenhouse light environment of the partly opaque roof. The study outlined a system combining a solar still with a controlled greenhouse environment and presented the mathematical description of the system performance. Furthermore, very few results are reported concerning light transmission through greenhouse roofs completely covered by flowing water. The effect of a water layer on light transmission and reflection was discussed by Morris *et al.* (1958) and Cohen *et al.* (1983) in connection with fluid roof systems for evaporative cooling of greenhouses. Heinemann and Walker (1987) studied the effects on light transmission of solar heating of water on the greenhouse cover surface. These studies indicate that the presence of a thin water film slightly increases the transmission of photosynthetic active radiation but also significantly decreases the infrared light transmission.

1.2. *Objectives and work stages*

This paper presents experimental and modelling results dealing with the influence of cover material optical properties on crop growth performance. The objective of this study is to present the measured spectral composition of the radiation, including the photosynthetically active radiation (PAR), transmitted through an experimental roof module for water desalination equipped with a specific absorber layer and operated with a water layer. These measurements are compared to simulations based on a spectral model of the optical transmission of the roof. A more general analysis includes theoretical sensitivity analysis for light transmission and related crop yield.

The work were carried out on a small roof desalination module. This module was used during a short period of intensive experiments under artificial light in a solar simulator at the laboratory of the Department of Buildings and Energy, Technical University of Denmark. The objective was to analyse the thermal and optical performance in controlled conditions (Chaibi, 2002) and to test and adjust the equipment to be used.

2. Materials and methods

2.1. *Experimental facilities*

The design of the solar desalination module is based on a rectangular box (2 m by 1 m), containing a flowing

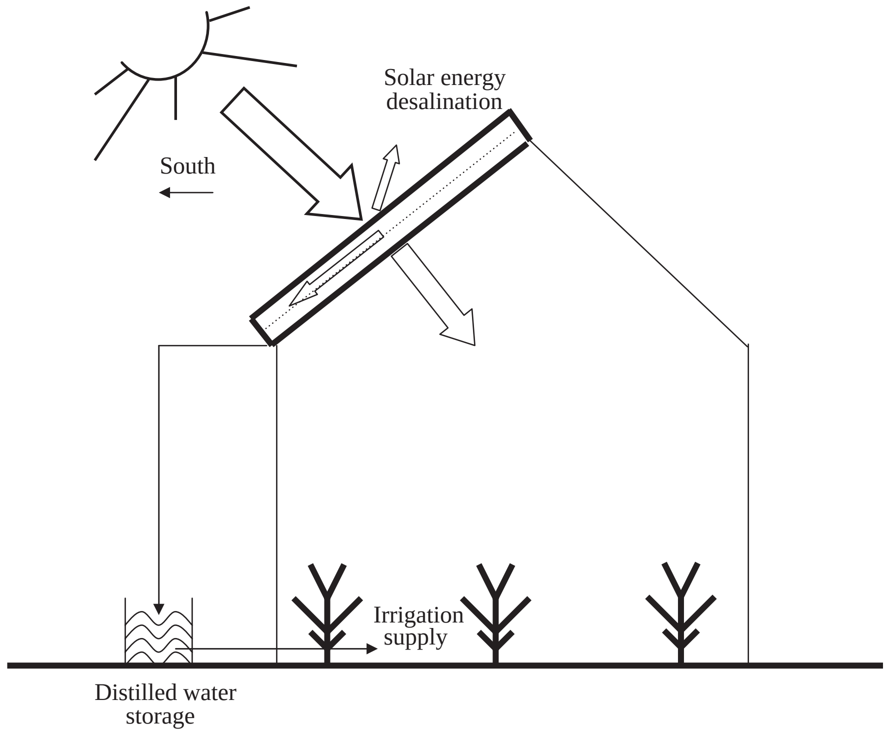

Fig. 1. Principle of a water desalination system integrated in a greenhouse roof

water layer at a fixed thickness (*Fig. 2*). The box has two cover material layers, a clear glass sheet at the top and a semi-transparent glass sheet on the bottom. The edges of the box are sealed and thermally insulated in order to minimise vapour and heat losses. The module is connected to equipment for water supply and collection, water storage and water flow control. All the equipment has been designed to be mobile in an easy way and has plan dimensions to fit on standard greenhouse roofs.

The laboratory experiment was arranged in an indoor solar simulator consisting of 64 compact source iodide (CSI) lamps at an average radiation level of about $560\,W\,m^{-2}$ on the top glass surface. More details at the design of the roof module are given in Chaibi (2002).

The water circulation system connected to the module secured a constant and well-controlled flow rate by using a water valve. The average solar intensity was determined using mobile pyranometers for measurements in a 0·1 m by 0·1 m grid at the level of the top glass before and after each measurement. The maximum long term drift of the artificial light was $\pm 0{\cdot}2\%$ and the uniformity over the measuring area was $\pm 15\%$ of the average value. The pyranometer inaccuracy was about 2·5% (Duer, 1999).

Measurements of the spectral distribution of the lamp irradiation (*Fig. 3*) and the spectral transmission of the roof materials were made with a spectroradiometer (Licor-1800 monochromator). The monochromator, working in the wavelength range 300–1100 nm, is driven by a precision step motor controlled by an internal microcomputer. The radiation intensity was measured for spectral intervals of 2 nm. The angle between the light beam and the plane of the glass surface was fixed at 36°.

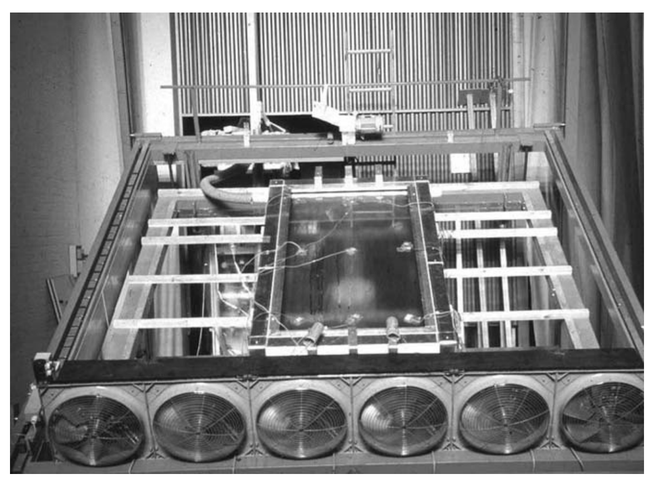

Fig. 2. Laboratory experiment with solar desalination module

The absorber was single glass, coated with a thin solar protection film. According to the manufacturer's specifications, the total solar and PAR absorption of this coated glass is around 56 and 53%, respectively.

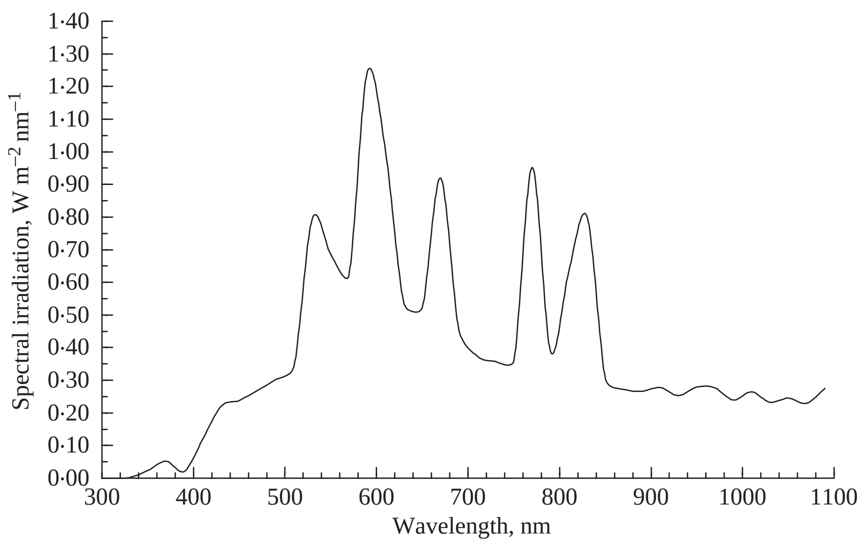

Fig. 3. Measured spectral distribution of the lamp irradiation in the solar simulator at the Technical University of Denmark; radiation level on the top glass surface of the experiment roof module

2.2. *Basis of the models*

2.2.1. *Light transmission model*

The incident solar radiation on the upper surface of the roof top glass is partly reflected upwards and partly refracted and transmitted towards the lower glass–air interface (*Fig. 4*). The beam incoming at the surface of a glass sheet separating two optical media, here air ($_a$) and glass ($_g$), is reflected from the surface at the same angle relative the surface normal as the incident beam θ_a. The remaining fraction enters the surface of the sheet at an angle θ_g determined by the indices of refraction n_a and n_g. This angle is calculated from Snell's law of refraction (Shand, 1958):

$$n_a \sin \theta_a = n_g \sin \theta_g \tag{1}$$

The refractive index is wavelength dependent, but for practical purposes the variation in the index can be considered negligible through the range of PAR (Duffie & Beckman, 1991).

The fraction of incident light reflected from the upper surface of the transparent glass r_g is determined from the average reflection coefficient for the parallel $r_{pa,g}$ and perpendicular $r_{pe,g}$ component of the polarised beam:

$$r_g = (r_{pa,g} r_{pe,g})/2 \tag{2}$$

where

$$r_{pa,g} = [\tan(\theta_a - \theta_g)/\tan(\theta_a + \theta_g)]^2 \tag{3}$$

$$r_{pe,g} = [\sin(\theta_a - \theta_g)/\sin(\theta_a + \theta_g)]^2 \tag{4}$$

The remaining light (*i.e.* the fraction, $1-r_g$) is either transmitted through the glass, absorbed, or reflected internally.

The transmission $\tau_{rl,g}$ through the top cover glass when only multiple reflection losses at the upper and lower glass surface are considered is calculated following Duffie and Beckman (1991):

$$\tau_{rl,g} = 1/2[(1 - r_{pa,g})/(1 + r_{pa,g})] + 1/2[(1 - r_{pe,g})/(1 + r_{pa,g})] \tag{5}$$

Absorption of the light by the top glass further reduces the transmittance. The transmitted fraction $\tau_{al,g}$, when only absorption losses are considered, is determined by Bouger's law

$$\tau_{al,g} = e^{-\beta_g (l_g/\cos\theta_g)} \tag{6}$$

where β_g is the extinction coefficient for the glass material in m^{-1}. The parameter l_g in m represents the glass thickness where $l_g/\cos\theta_g$ is the path length through the glass. The extinction coefficient is a function of properties of the material and wavelength but for practical applications, it is usually considered to have a constant value in the whole PAR spectrum.

For high-quality glass, β_g has a value of about $4\,m^{-1}$. This is a typical value for the so-called 'water white' glass (Duffie & Beckman, 1991) and the value is relevant for the whole PAR spectrum. For a poor-quality glass, which is slightly green coloured, the value of β_g to around $32\,m^{-1}$ (Duffie & Beckman, 1991).

The total transmission for the top glass is

$$\tau_g = \tau_{rl,g}\tau_{al,g} \tag{7}$$

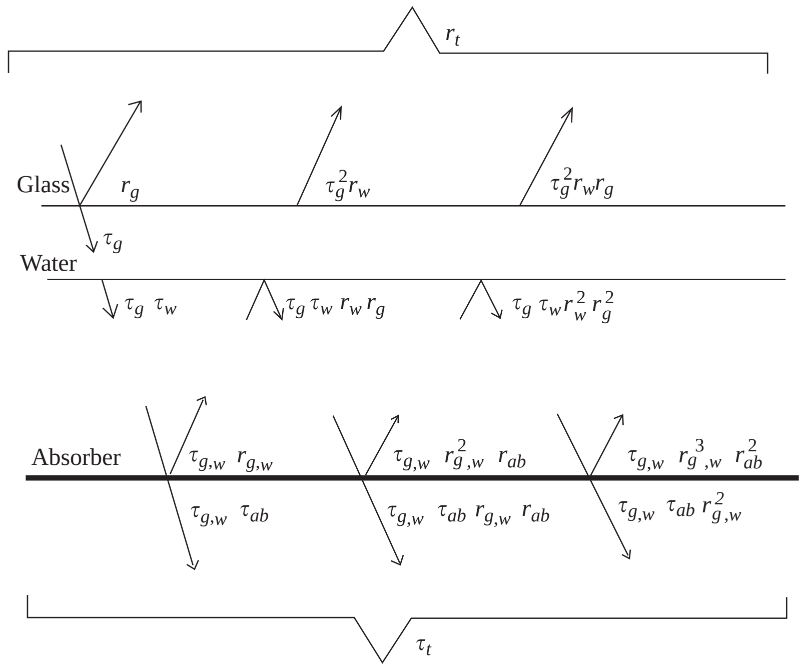

Fig. 4. Principal calculation of radiation transmission components with regard to absorption and multiple reflections in the glass, water and absorber layer of the roof: τ_t, the total roof transmission for a specified wavelength interval; r_t, the total reflection for a specified wavelength interval; subscripts g,w and ab, glass, water and absorber layers

The light transmitted through the glass is further attenuated when it reaches the film of water, placed between the two optical media glass and the transparent absorber material. The transmitted light is submitted to multiple reflections and shown in *Fig. 4*.

The total transmission coefficient $\tau_{g,w}$ for the combined glass and water layer can be expressed as a function of single layer coefficients τ_i and r_i. This coefficient includes the unreflected radiation and the internally reflected radiation transmitted to the absorber layer (*Fig. 4*). The expression is

$$\tau_{g,w} = \tau_g \tau_w (1 + r_g r_w + r_g^2 \cdot r_w^2 + \cdots + r_g^n r_w^n) \tag{8}$$

where τ_w represents the total transmittance of the water layer. It is calculated as the product of the transmitted fraction when only absorption losses are considered and the transmission through the water layer when only multiple reflection losses at the upper water surface are considered. The equation for τ_w is

$$\tau_w = \tau_{al,w} \tau_{rl,w} \tag{9}$$

The transmission coefficient $\tau_{al,w}$ is calculated (Eqn 6)

$$\tau_{al,w} = \mathrm{e}^{-\beta_w (l_w / \cos\ \theta_w)} \tag{10}$$

where: β_w is the extinction coefficient for water; $l_w/\cos\theta_w$, is the path length; and l_w is the thickness of the water layer.

Similarity, $\tau_{rl,w}$ is calculated from (see Eqn 5)

$$\tau_{rl,w} = 1/2[(1 - r_{pa,w})/(1 + r_{pa,w})] + 1/2[(1 - r_{pe,w})/(1 + r_{pe,w})] \tag{11}$$

where $r_{pa,w}$ and $r_{pe,w}$ are determined by the same method used for the glass layer [Eqns (1–4)].

The resulting reflection coefficient for the combined top glass and water layer is given by Jaffrin and Maklouf (1990)

$$r_{g,w} = (r_g + r_w - 2 r_g r_w)/(1 - r_g r_w) \tag{12}$$

When the transmitted light reaches the water–absorber interface, a third process of multiple reflection and absorption occurs. As in previous cases, the total transmittance of the absorption layer, and the fraction of incident light reflected from the upper surface of the absorption layer to the water are given by

$$\tau_{ab} = \mathrm{e}^{-\beta_{ab} (l_{ab} / \cos\ \theta_{ab})} \tag{13}$$

$$r_{w,ab} = (r_w + r_{ab} - 2 r_w r_{ab})/(1 - r_w r_{ab}) \tag{14}$$

The total transmission through the three layers of the roof, for a specified wavelength interval, is given by the following expression:

$$\tau_t = \tau_{g,w} \tau_{ab} (1 + r_{g,w} r_{ab} + r_{g,w}^2 r_{ab}^2 + \cdots + r_{g,w}^n r_{ab}^n \tag{15}$$

Consequently the total reflection of the roof for a specified wavelength interval is expressed as

$$r_t = 1 - (\tau_t + \alpha_t) \tag{16}$$

where α_t represent the sum of the absorption at the absorber level α_{ab}, water α_w and glass α_g layer.

The calculated total transmission and reflection in Eqns (15) and (16) only considers the direct radiation. The diffuse radiation is treated as a beam radiation with an equivalent angle of incidence of 64° (Kimball, 1973). In the following simulations of light transmission, the diffuse irradiation has been assumed to be 30% of the global irradiation. This is a typical value for the seasonal weather conditions in Mediterranean areas (Ghrab-Morcos & Ben Alaya, 1985).

The total transmittance τ_t of the roof is determined by the following equation:

$$\tau_t = \frac{\int_{\lambda=300}^{\lambda=400} I(\lambda)\tau_t(\lambda_{UV})\,\mathrm{d}\lambda + \int_{\lambda=400}^{\lambda=700} I(\lambda)\tau_t(\lambda_{PAR})\,\mathrm{d}\lambda + \int_{\lambda=700}^{\lambda=1100} I(\lambda)\tau_t(\lambda_{NIR})\,\mathrm{d}\lambda}{\int_{\lambda=300}^{\lambda=1100} I(\lambda)\,\mathrm{d}\lambda} \tag{17}$$

where the integrals of the energy $I(\lambda)\,\mathrm{d}\lambda$ for the ultraviolet (UV, 300–400 nm), the photosynthetically active (PAR, 400–700 nm) and the near infrared radiation (NIR, 700–1100 nm) are taken into account.

Table 1
Assumed extinction coefficients for saline water for applications and spectral intervals related to this study; data from Kanayama and Baba (1988) and Mertens (1970)

Wavelength interval (λ), nm	*Extinction coefficient (β), m^{-1}*
360–400	0·053
400–700	0·040
700–750	0·308
750–900	2·470
900–1200	17·400

The parameters τ_t for each wavelength band are solved using Eqns (1)–(15). The resolution was carried out by means of the Engineering Equation Solver (EES) computer program (Klein & Alvarado, 1997).

Simulations were carried under the assumption of an extinction coefficient β_g for glass of 16 m^{-1}. This value represents glass of modest quality. For saline water, and applications related to this study, the assumed extinction coefficient for several wavelength intervals is presented in Table 1.

The thickness of the glass sheets and the water layer flowing down the roof is assumed to be 4 and 2 mm, respectively. The index of refraction for glass is assumed to be 1·52 and for water 1·33.

As the considered application is related to greenhouse cultivation, the study is focused especially on the PAR light transmission. Under artificial light in the laboratory, the spectral light transmission for the film-coated glass used as absorber in the experimental roof module has been measured (Table 2). The absorber has a PAR transmission of about 23·5%.

Table 2 shows that the green/yellow and red light transmission was 24·9 and 25·7% while the transmission was about 5% lower for blue light. The transmission in the NIR spectrum was about 7% below the total PAR transmission.

2.2.2. *Crop growth*

The dynamic growth model of van Henten (1994) for the lettuce crop has been used in this work for simulation of plant yields. In this model, the growth rate is a function of climate parameters as the flux of photosynthetically active radiation, the carbon dioxide concentration of the air, and the greenhouse air

Table 2
Laboratory measured spectral transmission properties of the separate absorber solar protection film coated on a 4 mm glass sheet; transmission values for photosynthetically active radiation are expressed for each wavelength interval; blue light, λ = 400–500 nm; green/yellow light, λ = 500–650 nm; red light, λ = 650–700 nm

Total UV transmission coefficient ($\tau_{t,UV}$) λ = 300–400 nm)	*Total PAR transmission coefficient ($\tau_{t,PAR}$) (λ = 400–700 nm)*			*Total IR transmission coefficient ($\tau_{t,IR}$), λ = 700–1100 nm)*
	Blue light	*Green/yellow light*	*Red light*	
0·070	0·198	0·249	0·257	0·165

UV, ultraviolet; IR, infrared.

temperature. The two sub-models for the greenhouse micro-climate and the crop growth were structured and integrated in a clear and feasible way, allowing process state variables as well as system control actions to be simulated and inter-connected on a short-time basis. Consequently, this model appears to provide a useful tool for the prediction of plant growth under varying and limited environmental resources.

3. Experimental results and model validations

3.1. *Effect of a flowing water layer on spectral light transmission*

Spectral transmission measurements (300–1100 nm) in the laboratory for the inclined module with and without water flowing down the film-coated glass absorber are shown in *Fig. 5*. The transmission expressed in absolute % units increases by about 2%, for the PAR interval between 300 and 700 nm with a water layer when compared to the case without water on the absorber. A transmission decrease of about 5% is found for the NIR interval 700–1100 nm. The measured PAR transmission increase is close to the values reported by Pollet and Pieters (1999), Pieters (1996) and Jaffrin and Morisot (1994), who indicated that film condensation on plastic films causes transmittance gains of about 2·5%. The result was found through detailed analysis of plastic films transmission with water condensation on the inner surface. In addition, it can also partly be explained by the transmission spectrum for water which is nearly transparent for wavelengths between 400 and 800 nm. The water layer on the absorber decreases the total reflection losses for the roof. This effect is well known and is due to the fact that water is a medium having a refractive index value between the value of the absorber glass material and of the air, that reduces light losses through partial reflection at the upper glass surface. Above 700 nm the thin layer of water partly absorbs the radiation while the total transmittance for the near infrared light decreases considerably compared to the system without water. These result was confirmed by Morris *et al.* (1958) who studied the effects of a water layer on light transmission and reflection in connection with fluid roof systems for evaporative cooling of greenhouses. In this work, it was found that the presence of water on the roof had no significant effect on light transmission for the wavelength interval between 400 and 850 nm, while over 50% of the radiation between 1000 and 1400 nm was absorbed.

3.2. *Effect of the glass on transmission of photosynthetically active radiation for complete roofs*

In order to illustrate the effect of the top glass extinction coefficient β_g on the PAR transmission, calculations for the complete roof have been compared to the measured transmission, the results are presented in *Fig. 6*, for a case with water flow on the absorber with

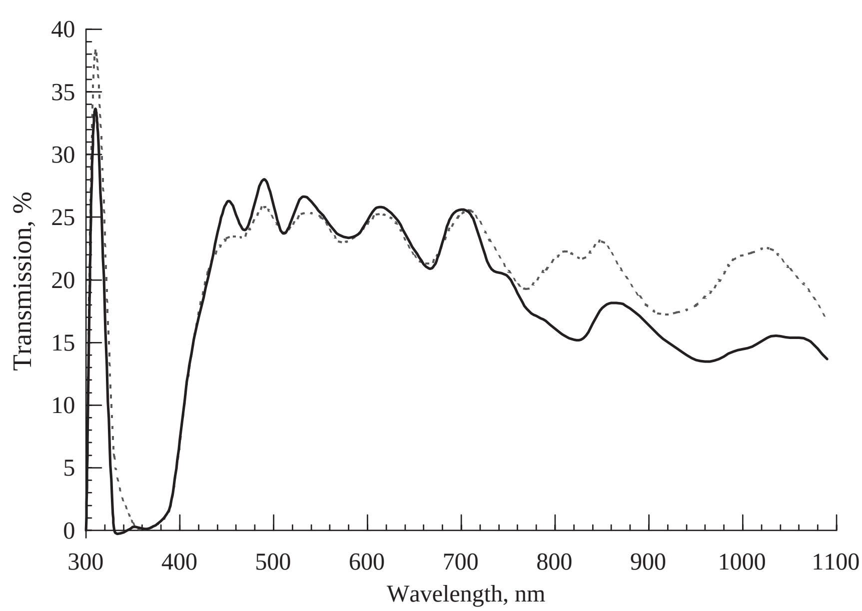

Fig. 5. Measured spectral transmission in the solar simulator for the complete roof with and without water flow on the absorber; the glass thickness is 4 mm and the water layer thickness about 2 mm: ……, without flow; ——, with flow

values for β_g of 5, 15 and $20\,m^{-1}$. Calculations were based on Eqn (15) where optical properties for the water and the absorber from Tables 1 and 2 are used. However, additional spectral data to those presented in Table 2 were used for derivation of the curves presented in *Fig. 6*.

A first and general observation is the close agreement in the whole spectrum between calculations and measurements. This validates the assumption of the model that the extinction coefficient for glass has a constant value in the whole PAR spectrum.

Table 3
Simulated transmission of photosynthetically active radiation (*PAR*) through complete roof with and without water flow and differences between simulated and measured values; variation of the top glass extinction coefficient β_g; glass thickness l_g, 4 mm and water layer thickness l_w, 2 mm

Glass extinction coefficient (β_g), m^{-1}	*Total PAR transmission coefficient $\tau_{t,PAR}$*		*Difference, %*
	Observed	*Simulated*	
Complete roof with water flow			
5	0·262	0·248	5·3
15	0·248	0·242	2·6
20	0·199	0·216	−8·5
Complete roof without water flow			
5	0·274	0·250	8·7
15	0·258	0·243	5·7
20	0·213	0·221	−3·7

The results for this case and the one without water flow on the absorber are shown in Table 3. For the water flow case, the best fit between calculation and measurement was found for β_g equal to $15\,m^{-1}$, which represents a rather low-quality glass. Without water flow, a value for β_g of $20\,m^{-1}$ gives the best fit. With regard to the NIR transmission, the best fit was found for the same values of β_g. The lower glass extinction coefficient due to the water flow in the NIR band is probably explained by the reduced reflection at the lower top glass surface owing to a thin condensate layer. However, this mechanism is not taken into account in the simulation model. The general conclusion of this analysis is that a nominal value of β_g for a low-quality glass used in this application should be reduced by about $5\ m^{-1}$ in order to get relevant PAR transmission simulation results.

4. Sensitivity analysis

The experiments and simulations concerning roof light transmission and crop growth were performed for a specific roof design and greenhouse climate. In this section, a more general analysis focused on seasonal crop yield variations for desalination roofs is presented. Included are yield analyses for variations of important optical material parameters and internal climate parameters. A conventional greenhouse without roof desalination was taken as reference.

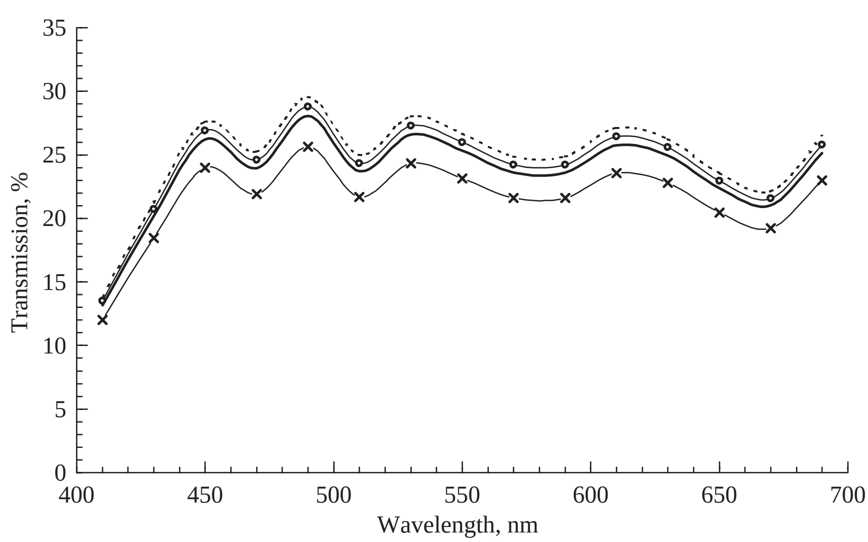

Fig. 6. Simulated compared to measured transmission of photosynthetically active radiation (PAR) in the solar simulator with water flow on the absorber; variation of the extinction coefficient (β_g) for the top glass material; the glass thickness is 4 mm and the water layer about 2 mm: ——, measured; ……, simulated ($\beta_g = 5\,m^{-1}$); —○—, simulated ($\beta_g = 15\,m^{-1}$); —×—, simulated ($\beta_g = 20\,m^{-1}$)

4.1. *Crop, climate and system parameters*

General assumptions in all analyses are the following:

(1) solar irradiation and ambient temperature for average, hourly conditions 1975–1979 (Ghrab-Morcos & Ben Alaya, 1985);
(2) diffuse irradiation as 30% of global radiation and PAR as 50% of global irradiation;
(3) desalination greenhouse with an asymmetrical roof with slope of 26° and oriented east–west;
(4) conventional greenhouse with single glass roof and the same geometry;
(5) low-quality glass with thickness of 4 mm and extinction coefficient of $16\,m^{-1}$ and considering only PAR transmission through the roof;
(6) CO_2 concentration in greenhouse air of 330 ppm and diurnal mean temperature in the air of 13°C, this temperature representing the mean value during the winter period as simulated with a greenhouse climate model (Chaibi & Jilar, 2004);
(7) lettuce crop, with a plant density of 10 plants m^{-2}; and
(8) dry weight assumed to be 5% of the fresh weight (Heuvelink & Challa, 1989).

4.2. *Crop yield as a function of light transmission and absorber absorptance*

The seasonal crop yield is analysed for a variation of the absorber absorptance between 5 and 80%. The single glass of the conventional greenhouse roof has an absorptance of about 5%.

In *Fig. 7*, the yield is shown as a function of the seasonal PAR light transmission. According to this curve a typical yield reduction of about 1% per % light reduction is found for the lower light transmission levels corresponding to the higher absorptance levels for desalination cases. For the higher light transmission levels corresponding to the conventional greenhouse, the yield reduction is about 0·5% per % light reduction. These results are confirmed by the analyses of Benoit and Ceustermans (1981) and Cockshull (1992) who reported yield reductions between 0·5 and 3·1% per % light reduction.

The relationship between yield and absorber absorptance is presented in *Fig 8*. For the actual climate conditions, a desalination roof with absorber absorptance of around 60% has the capacity to cover the fresh water demand for irrigation of a lettuce crop according to simulations with a water desalination model (Chaibi, 2000). For this case, a yield reduction of about 25% in relation to the conventional greenhouse case is found, as indicated in *Fig. 8*.

4.3. *Yield variation as influenced by top glass extinction and reflectivity*

The seasonal yield for variations of the extinction coefficient and the reflectivity of the top glass is shown in *Fig. 9*. The relative impact of the glass light extinction is logically high for higher absorber absorptance. For

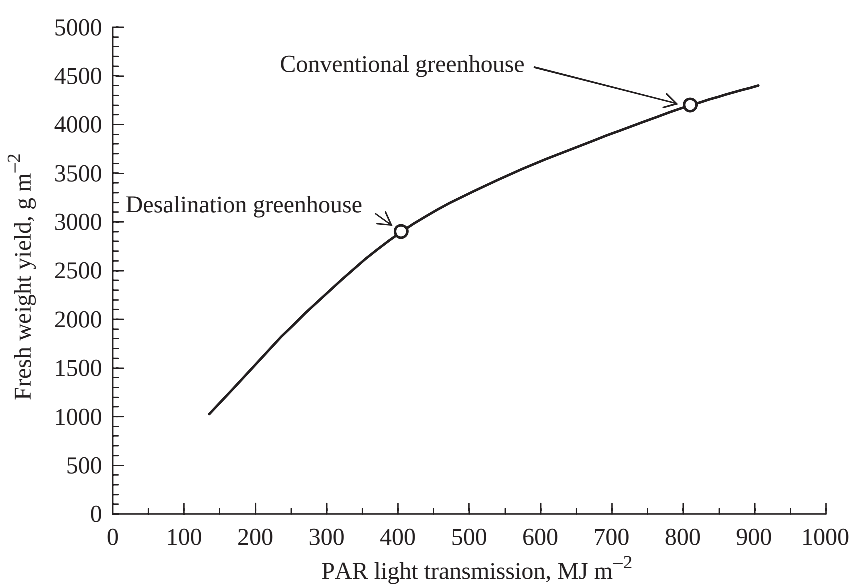

Fig. 7. Simulated seasonal lettuce crop yield as a function of seasonal transmission of photosynthetically active radiation (PAR) (horizontal) in Tunisian climate; variation of the absorber absorptance between 5 (right) and 80% (left); asymmetrical greenhouse roof with 26° slope and low quality top glass

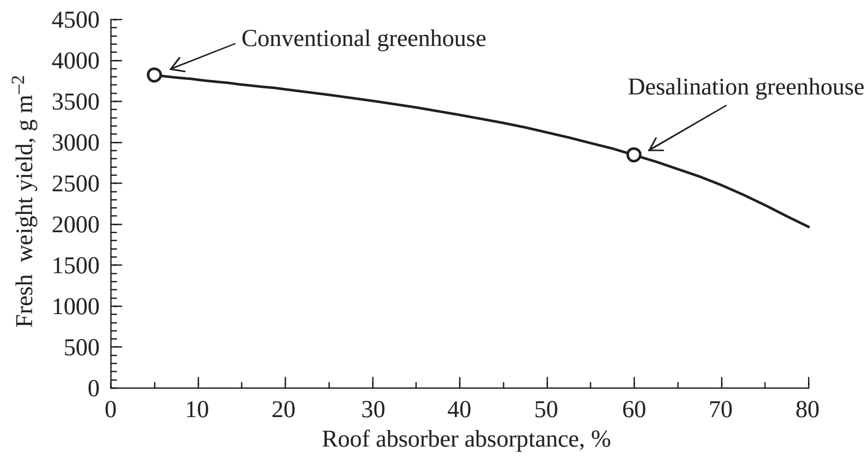

Fig. 8. Simulated seasonal lettuce crop yield as a function of absorber absorptance in Tunisan winter climate. Variation of the absorber absorptance between 5 (left) and 80% (right); asymmetrical greenhouse roof with 26° slope and low quality glass

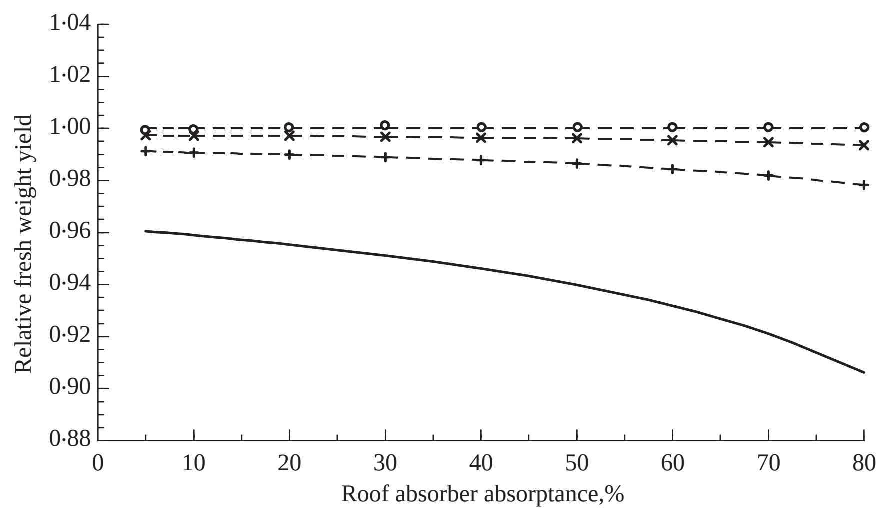

Fig. 9. Simulated relative seasonal lettuce crop yield as a function of absorber absorptance in Tunisian winter climate; variation of the top glass extinction (β_g) and reflectivity; asymmetrical greenhouse roof with 26° slope; the yield is related to the reference yield ($\beta_g = 16\,m^{-1}$) for each specific absorptance level: - -○- -, $\beta_g = 4\,m^{-1}$; - - × - -, $\beta_g = 8\,m^{-1}$; - -+- -, $\beta_g = 16\,m^{-1}$; ——, $\beta_g = 32\,m^{-1}$

instance, the desalination case with absorptance of 60% has a yield reduction of about 7% for low-quality glass ($\beta_g = 32\,\mathrm{m}^{-1}$) compared to a high 'water White' quality glass ($\beta_g = 4\,\mathrm{m}^{-1}$). The corresponding reduction is only 4% for the conventional greenhouse case.

5. Conclusions

From the model simulations and measurements of the solar radiation transmission through a desalination roof, the main conclusions are as follows.

(1) spectral of photosynthetically active radiation transmission (PAR) (300–700 nm) for complete roofs was simulated with high accuracy by the proposed model. The total PAR transmission is about 2% higher with water flow compared to a case without water.

(2) the model also describes accurately the spectral near infrared (NIR) transmission, where the total transmission is about 5% lower with water compared to without water.

(3) in order to account for reduced reflection losses due to internal condensation on the top glass, the glass extinction coefficient has to be reduced in the case of water flow.

A more general simulation analysis of seasonal crop yields for desalination compared to conventional greenhouses in arid climates indicates that

(4) the yield reduction is about 25% for a desalination case with the capacity to cover the water demand corresponding to a lettuce crop. This observations suggests the possibility of a more comprehensive climatic management and water production offered by the integrated solar desalination roof greenhouse, namely that the criterion for selecting solar desalination roof should ultimately be a question of maximising economic return for the grower. Future work should be directed at validating the absolute values of the performance energy and water consumption and crop yields in such systems.

Acknowledgements

The work was supported by grants from the Swedish Institute. The author gratefully acknowledges the staff of the Department of Buildings and Energy, Technical University of Denmark, especially Professor S. Svendsen and Dr. I. Holk, for the disposition of and help with laboratory resources.

References

Baille M; Baille A; Tchamitchian M (1990). A simple model for the estimation of greenhouse transmission: influence of structures and internal equipment. Acta Horticulturae, **281,** 35–46

Baille A; Mermier M; Baille M (1987). Greenhouse cover light transmission: an overview of French work. French-Israeli Symposium on Greenhouse Technology, Israel, pp 58–77

Benoit F; Ceustermans N (1981). Energy saving with Hortiplus glass. Acta Horticulturae, **107,** 59–63

Chaibi M T (2000). Analysis by simulation of a solar still integrated in a greenhouse roof. Desalination, **128,** 123–138

Chaibi M T (2002). Validation of a simulation model for water desalination in a greenhouse roof through laboratory experiments. Desalination, **142,** 65–78

Chaibi M T; Jilar T (2004). System design, operation and performance of roof-integrated desalination in greenhouses. Solar Energy, **76,** 545–561

Cockshull K E (1992). Crop environments. Acta Horticulturae, **312,** 77–83

Cockshull K E; Graves C J; Cave C R J; Carol R J (1992). The influence of shading on yield of glasshouse tomatoes. Journal of Horticulture Science, **67**(1), 11–24

Cohen Y; Stanhill G; Fuchs M (1983). An experimental comparison of evaporative cooling in a naturally ventilated glasshouse due to wetting the outer and inner crop soil surfaces. Agriculture Meteorology, **28,** 239–251

Critten D L (1983). A computer model to calculate the daily light integral and transmissivity of a greenhouse. Journal of Agricultural Engineering Research, **28,** 61–76

Duer K (1999). Performance of a solar collector with antireflection treated glass cover. Department of Buildings and Energy, Technical University of Denmark, Report SR 99-14, 11pp

Duffie J A; Beckman W A (1991). Solar Engineering of Thermal Processes, (2nd Edn). A Wiley Interscience Publication, New York, USA

Ghrab-Morcos N; Ben Alaya H (1985). Données climatiques de Tunis pour l'application de l'énergie solaire dans le bâtiment. [Climatic data in Tunis for solar energy application in building.] ENIT Solar Energy Laboratory, Internal Note No 85/1, p 78

Heinemann P H; Walker P N (1997). Effects of greenhouse surface heating water on light transmission. Transactions of the ASAE, 215–220

Heuvelink E P; Challa H (1989). Dynamic optimization of artificial lighting in greenhouses. Acta Horticulturae, **260,** 401–412

Holder R; Cockshull K E (1990). The effects of humidity on the growth and yield of glass house tomatoes. Journal of Horticulture Science, **65,** 31–39

Jaffrin A; Makhlouf S (1990). Mechanism of light transmission through wet polymer films. Acta Horticulturae, **281,** 11–24

Jaffrin A; Morisot A (1994). Role of structure, dirt and condensation on the light transmission of greenhouse covers. Plasticulture, **1,** 33–44

Kanayama K; Baba H (1988). Transmittance of distilled water and sodium-chloride-waters solutions. Journal of Solar Energy Engineering, **110,** 113–117

Kimball B A (1973). Simulation of the energy balance of a greenhouse. Agriculture Meteorology, **11,** 243–260

Klein S A; Alvarado F L (1997). EES Engineering Equation Solver. F-Chart Software, Wisconsin, USA

Kozai T (1977). Direct solar light transmission into multispan greenhouses. Agriculture Meteorology, **18,** 327–338

McMahon M J; Kelly J W; Decoteau D R (1990). Spectral transmittance of selected greenhouse construction and nursery shading material. Journal of Environmental Horticulture, **8**(3), 118–121

Mertens L E (1970). Underwater Photography. John Wiley Interscience, New York, USA

Morris L G; Trickett E S; Vanstone F H; Wells D A (1958). The limitation of maximum temperature in a glasshouse by the use of a thin film on the roof. Journal of Agricultural Engineering Research, **3,** 121–130

Mortensen L M; Stromme E (1987). Effect of light quality on some greenhouse crops. Scientia Horticulturae, **33,** 27–36

Nijskens J; de Halleux D; Coutisse S; Nisen A (1985). Radiation transfer through covering materials, solar and thermal screens of greenhouses. Agriculture Forest Meteorology, **35,** 229–242

Pieters J G (1996). Condensation and PAR transmission of greenhouses. Plasticulture, **4,** 23–31

Pollet I V; Pieters J G (1999). Laboratory measurements of PAR transmittance of wet and dry greenhouse cladding materials. Agriculture Forest Meteorology, **93,** 149–152

Raviv M (1989). The use of photoselective cladding materials as modifiers of morphogenesis of plants and pathogens. Acta Horticulturae, **246,** 275–284

Selcuk M K (1970). The effect of solar radiation on the energy balance of a controlled environment greenhouse. ASME Annual Winter Meeting, New York, Paper No. 70/WA/5063, pp 1–8

Shand E B (1958). Glass Engineering Handbook. McGraw-Hill Book, New York, USA

Tinault D; Echaniz G; Ramos F (1978). Materials for solar still greenhouse. Optica Pura Y Aplicada, **11,** 59–61

Van Henten E J (1994). Greenhouse climate management: an optimal approach. Dissertation, Wageningen Agricultural University, Wageningen, p 329